

Estimating bioturbation from replicated small-sample radiocarbon ages

Andrew M. Dolman¹, Jeroen Groeneveld^{1,2}, Gesine Mollenhauer^{3,4,5}, Sze Ling Ho⁶, Thomas Laepple^{1,4,5}

¹Alfred-Wegener-Institut Helmholtz-Zentrum für Polar-und Meeresforschung, 14473 Potsdam, Germany

²Institute of Geology, Hamburg University, 20146 Hamburg, Germany

³Alfred-Wegener-Institut Helmholtz-Zentrum für Polar-und Meeresforschung, 25570 Bremerhaven, Germany

Germany

⁴Department of Geosciences, University of Bremen, 28359 Bremen, Germany

⁵University of Bremen, MARUM – Center for Marine Environmental Sciences and Faculty of Geosciences, 28334 Bremen, Germany

⁶Institute of Oceanography, National Taiwan University, 10617 Taipei, Taiwan

Key Points:

- Age-heterogeneity within sediment layers adds hidden uncertainty to radiocarbon-based age estimates.
- The amount of age-heterogeneity depends on the sedimentation rate and bioturbation mixing depth.
- We present a method to estimate ¹⁴C age-heterogeneity and lookup figure to estimate age uncertainty.

Corresponding author: Andrew M. Dolman, andrew.dolman@awi.de

20 **Abstract**

21 Marine sedimentary records are a key archive when reconstructing past climate;
 22 however, mixing at the seabed (bioturbation) can strongly influence climate records, es-
 23 pecially when sedimentation rates are low. By commingling the climate signal from dif-
 24 ferent time periods, bioturbation both smooths climate records, by damping fast climate
 25 variations, and creates noise when measurements are made on samples containing small
 26 numbers of individual proxy carriers, such as foraminifera. Bioturbation also influences
 27 radiocarbon-based age-depth models, as sample ages may not represent the true ages of
 28 the sediment layers from which they were picked. While these effects were first described
 29 several decades ago, the advent of ultra-small-sample ^{14}C dating now allows samples con-
 30 taining very small numbers of foraminifera to be measured, thus enabling us to directly
 31 measure the age-heterogeneity of sediment for the first time. Here, we use radiocarbon
 32 dates measured on replicated samples of 3-30 foraminifera to estimate age-heterogeneity
 33 for five marine sediment cores with sedimentation rates ranging from 2-30 cm kyr^{-1} . From
 34 their age-heterogeneities and sedimentation rates we infer mixing depths of 10-20 cm for
 35 our core sites. Our results show that when accounting for age-heterogeneity, the true er-
 36 ror of radiocarbon dating can be several times larger than the reported measurement.
 37 We present estimates of this uncertainty as a function of sedimentation rate and the num-
 38 ber of individuals per radiocarbon date. A better understanding of this uncertainty will
 39 help us to optimise radiocarbon measurements, construct age models with appropriate
 40 uncertainties and better interpret marine paleo records.

41 **1 Introduction**

42 Proxy records recovered from sediments are an important source of information about
 43 the history of the Earth's climate prior to the instrumental era. For example, the ratio
 44 of magnesium to calcium (Mg/Ca) in the shells of marine organisms such as foraminifera
 45 contains information about the temperature of the environment in which calcification
 46 took place (Nürnberg et al., 1996; Lea, 2014; Rosenthal et al., 2000). These shells set-
 47 tle to the sediment surface and are buried as further sediment accumulates. Over time
 48 this produces an archive of recorded (proxy) temperatures that can be read in sequence
 49 by taking a sediment core and measuring the Mg/Ca ratio of shells found at progressively
 50 deeper, and therefore older, positions in the core.

51 To obtain a down-core proxy record, samples of foraminiferal shells (hereafter foraminifera)
 52 are picked from a series of sediment slices or down-core samples. Assuming, for exam-
 53 ple, that these slices are 1 cm thick and come from a core location with a constant sed-
 54 imentation rate of 5 cm kyr^{-1} , foraminifera from a single slice would have a uniform dis-
 55 tribution of ages with a width of 200 years, with a corresponding standard deviation (SD)
 56 of 58 years. However, wherever oxygenated, the surface layer of marine and freshwater
 57 sediments is mixed or bioturbated by the burrowing and feeding actions of benthic or-
 58 ganisms, thus increasing the age-heterogeneity of material at a given depth (Guinasso
 59 & Schink, 1975; Boudreau, 1998). For simple models of sediment mixing, the standard
 60 deviation of ages at a given depth is simply the ratio of the mixed depth L and the sed-
 61 iment accumulation rate s (Guinasso & Schink, 1975). For a core with a 5 cm kyr^{-1} sed-
 62 imentation rate and 10 cm bioturbation depth, $L/s = 2000$ years, and therefore bio-
 63 turbation greatly increases the expected age-heterogeneity of a sediment slice from 58
 64 to approximately 2000 years.

65 The additional age-heterogeneity created by bioturbation has important implica-
 66 tions for sedimentary proxy records. Proxies measured on samples containing multiple
 67 individual signal carriers (e.g. foraminifera) will represent means over the time periods
 68 that have been mixed together. This has a smoothing or filtering effect on any signal,
 69 so that the observed amplitude of climate variations is reduced (Anderson, 2001). In ad-
 70 dition to this smoothing effect, if proxies are measured on samples containing only a small

71 number of individual signal carriers, the resulting values will be noisy means of the cli-
 72 mate state over the time interval that has been mixed together (Schiffelbein & Hills, 1984;
 73 Kunz et al., 2020; Dolman et al., 2020). It would therefore be very useful to have an es-
 74 timate of the degree of age-heterogeneity when interpreting proxy climate records.

75 Radiocarbon dating is the principle method used to estimate the age of sediment
 76 material younger than about 50 ka BP. The age inferred from the measured radiocar-
 77 bon content is an estimate of the mean age of the particles in a given sample, and sim-
 78 ilarly, the reported machine error represents uncertainty in the mean age of the specific
 79 sample. However, the particles in a given sample are themselves only a sub-sample of
 80 the material from a given depth, and there is therefore additional, hidden, uncertainty
 81 about how representative the sample is of the age of the rest of the material from the
 82 same depth. Traditionally, radiocarbon dating required large samples of material that
 83 would necessarily include 100s of individual foraminifera (typically the equivalent of 1-
 84 5 mg C). Therefore, although it would give no indication of the heterogeneity in the age
 85 of the material, a single radiocarbon date would be a good estimate of the mean age of
 86 material at a given depth. However, the advent of ultra-small sample radiocarbon dat-
 87 ing (Wacker et al., 2010) means that samples consisting of very small numbers of foraminifera
 88 can now be dated. With fewer individuals per sample, radiocarbon measurements be-
 89 come noisier estimates of the mean age of material at a given depth. However, by radio-
 90 carbon dating replicated samples of just a few individual foraminifera we can use this
 91 "noise" to estimate the age-heterogeneity of the sediment and to aid our interpretation
 92 of proxy climate records.

93 As described above, assuming a simple sediment mixing model, age-heterogeneity
 94 can be estimated from the ratio of the mixing depth and sedimentation rate, L/s . How-
 95 ever, while the sedimentation rate for a given core can be readily determined using a se-
 96 ries of down-core radiocarbon dates, the mixing depth is harder to estimate. Direct mea-
 97 surements using particle tracers show that L is highly variable in space (8.37 \pm 6.19 cm,
 98 Teal et al., 2010) and mixing intensity may be particle size dependent (Wheatcroft, 1992;
 99 Thomson et al., 1995). Short life-span tracers, such as ^{210}Pb (half-life 26 years) may sim-
 100 ply miss sporadic mixing events that compound over time to produce the long-term mix-
 101 ing behaviour. Additionally, these direct estimates of mixing depth are rarely available
 102 at proxy record core sites and in any-case give an estimate of the current mixing depth
 103 and cannot inform us about mixing depths in the past when the sediment archive was
 104 formed. Mixing depth can also be inferred from the "kink" in a series of down-core ^{14}C
 105 measurements (e.g., Trauth et al., 1997), but this requires a large number of measure-
 106 ments in the first 0-20 cm of the sediment core, and for gravity and piston cores the up-
 107 per few centimetres are often lost during recovery. Although they integrate mixing over
 108 a longer time period than tracer experiments, kink based estimates also cannot tell us
 109 about mixing depths in the past.

110 Here we propose and test a method to directly estimate the age-heterogeneity of
 111 sediment by radiocarbon dating replicated samples of small numbers (3-30) of foraminifera
 112 and using the age-variation between these samples to estimate inter-individual age-heterogeneity.
 113 From this we can further infer bioturbation depths in these cores at the time the dated
 114 material was deposited. The wider use of this method would allow for a more rigorous
 115 interpretation of proxy climate records by providing direct estimates of age-heterogeneity
 116 and its smoothing effect on a per-core basis. The hidden uncertainty in radiocarbon based
 117 age-control points can also be estimated, resulting in better age-depth models. With this
 118 knowledge we can also further optimise future drilling campaigns sampling strategies.
 119 We examine the necessary conditions to use this method and estimate correction factors
 120 for the bias due to the exponential relationship between radiocarbon activity and age.

121 2 Materials and Methods

122 2.1 Physical Sampling and Radiocarbon Dating

123 We used foraminifera picked from five sediment cores recovered that span a range
 124 of sediment accumulation rates (approximately 2-30 cm kyr⁻¹). The sites were sampled
 125 as part of the SO184, SO213/2 and OR1-1218 cruises (Table 1, Figure 1) (Hebbeln &
 126 cruise participants, 2006; Tiedemann et al., 2014).

127 Radiocarbon dating was performed on samples of single species of foraminifera picked
 128 from discrete 1 cm thick sediment slices. With the exception of one sample from GeoB
 129 10066-7, a single species was used from each core, either *Globigerina bulloides* (SO213-
 130 84-2, 250-400 μm size fraction) or *Trilobatus sacculifer* without sac-like final chamber
 131 (GeoB 10054-4, GeoB 10058-1, GeoB 10066-7, 250-400 μm size fraction; and OR1-1218-
 132 C2-BC, 300-355 μm or 315-355 μm) (Table 2).

133 To estimate sediment age-heterogeneity, replicated "small-*n*" radiocarbon dates were
 134 measured on samples consisting of between three and thirty individual foraminifera, n_f ,
 135 with multiple replicate samples taken from each sediment slice, n_{rep} . We use the term
 136 "small-*n*" to refer specifically to samples consisting of a small number of discrete par-
 137 ticles, or individuals, rather than samples with a small mass of carbon, but which may
 138 contain parts from a great many individuals. Additional radiocarbon dating was per-
 139 formed on non-replicated "bulk" samples consisting of larger numbers of foraminifera,
 140 to provide down-core age control points for estimating sediment accumulation rates. With
 141 the exception of the bulk samples from core SO213-84-2, all Accelerated Mass Spectrom-
 142 etry (AMS) ¹⁴C dates were generated using a Mini Carbon Dating System (MICADAS)
 143 at the Alfred Wegener Institute, Bremerhaven, Germany (Wacker et al., 2010). MICADAS'
 144 capability of analysing a gas target was used for small-*n* samples (Ruff et al., 2010), larger
 145 samples were measured using a graphite target. Radiocarbon dating of the bulk sam-
 146 ples from core SO213-84-2 was carried out at NOSAMS, Woods Hole Oceanographic In-
 147 stitution and Keck Carbon Cycle AMS Laboratory, University of California, Irvine.

148 Radiocarbon dates were converted to calendar ages using the Marine13 calibration
 149 (Reimer et al., 2013) and the R package Bchron (Haslett & Parnell, 2008). The Marine13
 150 calibration includes a time-varying global marine reservoir effect. We did not adjust for
 151 local marine reservoir effects as this should not influence the variance in ages found in
 152 a given sediment slice. For each sample, the probability density function (PDF) for cal-
 153 endar age was summarised by its mean and standard deviation, as none of the PDFs were
 154 bi- or multi-modal.

155 Sediment accumulation rates were estimated by linear regression of calibrated cal-
 156 endar age on depth. Bulk and small-*n* dates from the depth range 15-100 cm (10-37 cm
 157 for OR1-1218-C2-BC) were used so as to exclude the mixed layer and to estimate the
 158 sediment accumulation rate over the range of depths for which replicated ¹⁴C measure-
 159 ments were made. For replicated small-*n* dates, a mean date was first calculated for each
 160 depth. The multicore GeoB 10058-1 and gravity core GeoB 10054-4 were intended to be
 161 taken at the same site, but due to technical difficulties were in fact taken on subsequent
 162 days at locations 3 km apart (Hebbeln & cruise participants, 2006). However, their down-
 163 core radiocarbon data indicate very similar sedimentation rates (approximately 16 cm
 164 kyr⁻¹) and we combined these to create a single more robust sedimentation rate esti-
 165 mate.

166 2.2 Estimation of Age-Heterogeneity

167 For each sediment slice, we calculated the variance between replicated calendar age
 168 estimates, σ_{rep}^2 . From this we subtracted the mean measurement error reported by the
 169 MICADAS lab for samples from that slice, σ_{meas}^2 . As the ages of the individuals are in-

Table 1. Sediment cores used in this study with their locations and the research cruise during which the core was taken.

Core	Cruise	Latitude	Longitude	Water depth [m]
GeoB 10054-4	SO184	8°40'54"S	112°40'6"E	1076
GeoB 10066-7	SO184	9°23'33.6"S	118°34'31.8"E	1635
OR1-1218-C2-BC	OR1-1218	10°54'1.8"N	115°18'27.6"E	2208
GeoB 10058-1	SO184	8°40'S	112°38'E	1103
SO213-84-2	SO213/2	45°7'28.2"S	174°35'11.4"E	992

Table 2. Summary of radiocarbon dating per core and depth. Sub-core or tube is indicated in parentheses when appropriate. n_f is the number of individual foraminifera per radiocarbon dated sample, n_{rep} is the number of replicated radiocarbon dated samples.

Core	Core depth [cm]	Species	Size fraction [μm]	n_f	n_{rep}
GeoB 10054-4	28-29	<i>T. sacculifer</i>	250-400	50	1
GeoB 10054-4	48-49	<i>T. sacculifer</i>	250-400	50	1
GeoB 10054-4	68-69	<i>T. sacculifer</i>	250-400	10	10
GeoB 10054-4	88-89	<i>T. sacculifer</i>	250-400	50	1
GeoB 10058-1	11-12	<i>T. sacculifer</i>	250-400	5-6	20
GeoB 10058-1	17-18	<i>T. sacculifer</i>	250-400	110	1
GeoB 10058-1	20-21	<i>T. sacculifer</i>	250-400	110	1
GeoB 10058-1	23-24	<i>T. sacculifer</i>	250-400	110	1
GeoB 10058-1	26-27	<i>T. sacculifer</i>	250-400	110	1
GeoB 10058-1	29-30	<i>T. sacculifer</i>	250-400	5-6	20
GeoB 10066-7	23-24	<i>T. sacculifer</i>	250-400	50	1
GeoB 10066-7	48-49	<i>T. sacculifer</i>	250-400	49	1
GeoB 10066-7 ^a	53-54	<i>G. bulloides</i>	250-400	10	10
GeoB 10066-7	98-99	<i>T. sacculifer</i>	250-400	53	1
OR1-1218-C2-BC (1)	36-37	<i>T. sacculifer</i>	315-355	5	10
OR1-1218-C2-BC (1)	36-37	<i>T. sacculifer</i>	300-355	30	1
OR1-1218-C2-BC (1)	36-37	<i>T. sacculifer</i>	315-355	200	3
OR1-1218-C2-BC (7,8,9)	10-12	<i>T. sacculifer</i>	315-355	200	6
SO213-84-2 (1)	1-2	<i>G. bulloides</i>	250-400	5-6	10
SO213-84-2 (1)	18-19	<i>G. bulloides</i>	250-400	>350	1
SO213-84-2 (1)	23-24	<i>G. bulloides</i>	250-400	5-6	10
SO213-84-2 (1)	23-24	<i>G. bulloides</i>	250-400	>350	1
SO213-84-2 (2)	17-18	<i>G. bulloides</i>	250-400	>350	1
SO213-84-2 (2)	20-21	<i>G. bulloides</i>	250-400	>350	1
SO213-84-2 (3)	17-18	<i>G. bulloides</i>	250-400	>350	1
SO213-84-2 (3)	21-22	<i>G. bulloides</i>	250-400	3	12
SO213-84-2 (3)	21-22	<i>G. bulloides</i>	250-400	5-6	10
SO213-84-2 (3)	21-22	<i>G. bulloides</i>	250-400	30	8
SO213-84-2 (3)	22-23	<i>G. bulloides</i>	250-400	>350	1

^a *G. bulloides* were picked from a single slice from GeoB 10066-7

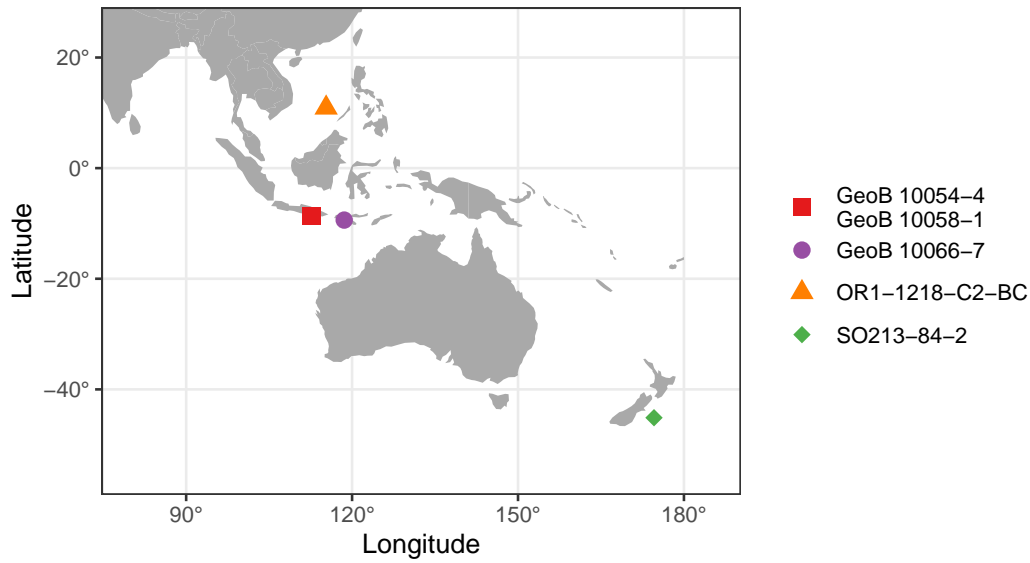


Figure 1. Locations of cores used in this study. Additional data published in Lougheed et al. (2018) from a core in the mid-Atlantic (29°59'150 W, 37°8'130 N) are included in the discussion but the core location is outside the range of this map and not shown. GeoB 10054-4 and GeoB 10058-1 are a gravity core and multicore respectively, taken at sites approximately 3 km apart.

170 dependent, the variance between individuals, σ_{ind}^2 , can be inferred as the variance be-
 171 tween replicates of size n_f multiplied by n_f .

$$172 \quad \sigma_{ind}^2 = n_f(\sigma_{rep}^2 - \sigma_{meas}^2) \quad (1)$$

173 The inter-individual variance contains a component from the finite sediment width
 174 τ_{slice} (here 1 cm) and additional variation due to sediment mixing. We can estimate the
 175 variance due to the slice thickness using equation (2), where the 1/12 comes from the
 176 formula for the variance of a uniform distribution. After subtracting the variance due
 177 to the slice thickness we attribute the remaining excess variance to bioturbation, assum-
 178 ing that the radiocarbon age during deposition was the same for all particles.

$$179 \quad \sigma_{slice}^2 = \frac{1}{12} \left(1000 \cdot \frac{\tau_{slice} \text{ [cm]}}{s \text{ [cm kyr}^{-1}\text{]}} \right)^2 \quad (2)$$

$$180 \quad \sigma_{bioturbation}^2 = \sigma_{ind}^2 - \sigma_{slice}^2 \quad (3)$$

181 To interpret this value, we use the simple bioturbation model proposed by Berger
 182 and Heath (1968) to infer a mixing depth from $\sigma_{bioturbation}^2$. Assuming that the upper
 183 L centimetres of sediment are fully and instantaneously mixed but below this level there
 184 is no further mixing, and in which the sedimentation rate and flux of foraminifera is as-
 185 sumed to be constant (Berger & Heath, 1968; Matisoff, 1982; Officer & Lynch, 1983),
 186 the bioturbation depth required to produce this excess age-variance is given by:

$$187 \quad L = \frac{s}{1000} \sqrt{\sigma_{bioturbation}^2} \quad (4)$$

188

2.3 Bias Correction

189

Due to the exponential relationship between age and radiocarbon activity, estimates of both mean age, and age-variance between multiple samples, are biased because younger individual particles contribute exponentially more to the mean $^{14}\text{C}/^{12}\text{C}$ ratio. When the underlying age distribution is exponential, and there are infinitely many particles in the sample, there is an analytical formula for the bias in the mean radiocarbon age (Andree, 1987), however, we are not aware of a general solution for finite sample sizes. To address this we carried out a Monte-Carlo simulation study to investigate the properties of this bias and to obtain correction factors to adjust our measured age-heterogeneity estimates.

197

198

199

200

201

202

203

204

205

206

207

208

We simulated the process of sampling foraminifera from discrete depths by sampling replicated sets of n_f foraminifera from an exponential age distribution with a standard deviation corresponding to a given combination of L and s . For the purpose of the simulation we ignored the difference between calendar and radiocarbon age and convert the age of each foraminifera to an $F^{14}\text{C}$ value with the expression $F^{14}\text{C} = e^{-\frac{age}{8033}}$. For each replicate of n_f foraminifera we then calculated its mean age and mean $F^{14}\text{C}$ value. Mean $F^{14}\text{C}$ values were then back-transformed to (radiocarbon) ages, $age_{F^{14}\text{C}}$. The standard deviation between mean age and mean $age_{F^{14}\text{C}}$ values were then calculated for the replicated groups. We repeated this process for a range of underlying age variances and for groups with differing number of foraminifera per $F^{14}\text{C}$ "measurement". The difference between the standard deviation in age and standard deviation in $age_{F^{14}\text{C}}$ represents the expected bias in estimates of age-heterogeneity.

209

210

211

212

213

214

215

216

217

To adjust for this underestimation of age-heterogeneity we calculated correction factors by which to multiply biased estimates of age-heterogeneity (Figure 2). These correction factors likely represent an upper limit on the potential bias, as the bias depends on the shape of the underlying age distribution. If the true age-distribution differs from the assumed exponential, it is probably less skewed than an exponential and hence would produce a smaller bias. In the results we present both adjusted and un-adjusted age-heterogeneities and implied bioturbation depths. The simulation was written in R code and carried out with R version 3.6.2 (R Core Team, 2019). For more detail see Supporting Text S1 and Figure S1.

218

3 Results

219

3.1 Age-Heterogeneity in Core SO213-84-2

220

221

222

223

224

225

226

227

228

229

230

231

We first examine radiocarbon dates from the multicore SO213-84-2, for which we made measurements on groups of 3, 6 and 30 individual foraminifera, all picked from a single depth of multicore tube 3 (21-22 cm). For samples of 30 individuals, calendar ages range from 7.50 to 9.93 ka BP, with a standard deviation (σ_{rep}) of 726 years, a value far greater than the reported measurement error of about 150 years. Variation in age between samples is even greater for replicates of 6 foraminifera (range = 6.57 - 12.23 ka BP, $\sigma_{rep} = 1514$ years) and 3 foraminifera (range = 4.32 to 13.99 years BP, $\sigma_{rep} = 2895$ years). Clearly, the calibrated calendar ages of these replicated samples do not agree with each other within their reported uncertainties and this excess variation decreases strongly with the number of foraminifera per measurement (Figure 3). Additional measurements on replicated samples of 5-6 individuals taken from multicore tube 1 at depths of 1-2 and 23-24 cm have similarly large σ_{rep} values of 1187 and 1575 years.

232

233

234

235

236

237

The relationship between σ_{rep} and the number of individuals per measurement very closely follows an inverse relationship (Figure 4). This is a strong indication that inter-individual age variation (σ_{ind}) is the major component of the between sample variation and allows us to infer σ_{ind} by scaling for the number of foraminifera per sample, after first subtracting the much smaller reported measurement error (Equation 1). Inferred age-heterogeneity between individuals, σ_{ind} , from core SO213-84-2 ranges from 2854 to

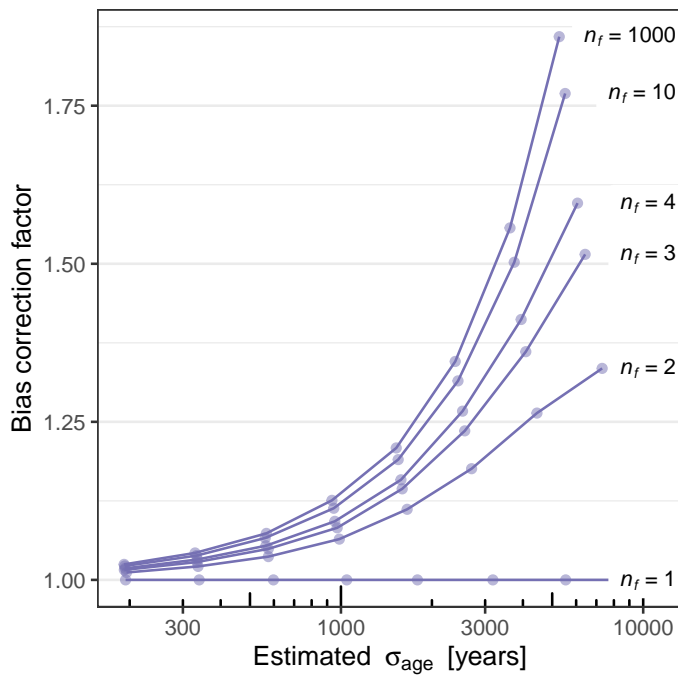


Figure 2. Bias correction factors to correct for the underestimation of age-heterogeneity due to the exponential relationship between radiocarbon activity and age.

238 4990 years (Table 3). Bias correction factors for SO213-84-2 estimated by simulation vary
 239 between 1.36 and 1.51, depending on the number of foraminifera per sample. Adjust-
 240 ing for the bias, the range of $\sigma_{ind_{adj}}^2$ increases to 3881 - 6847 years. Also shown in Ta-
 241 ble 3 is the much smaller age-heterogeneity of approximately 100 years expected due to
 242 the 1 cm thickness of the slice and the 2.9 cm kyr⁻¹ sedimentation rate. After subtract-
 243 ing this, and assuming a simple sediment mixing model (Berger & Heath, 1968), the ex-
 244 cess age-heterogeneity implies a mixing depth of 11.2 - 19.8 cm (8.3 - 14.4 before bias
 245 adjustment) (Equations 1-4, Table 3). Age-heterogeneity is somewhat lower for the sam-
 246 ples from 1-2 cm deep, which would be in the active mixing layer, than for the other deeper
 247 samples.

248 3.2 Age-Heterogeneity Across Multiple Cores

249 To test the generality of this result we performed similar replicated small-*n* radio-
 250 carbon measurements at 4 additional sites with sediment accumulation rates of approx-
 251 imately 2, 16 (2 sites), and 29 cm kyr⁻¹. We again adjust the measured age-heterogeneity
 252 for bias assuming an exponential age distribution and present both adjusted and un-adjusted
 253 age-heterogeneities and bioturbation depths for comparison. To examine the relation-
 254 ship between age-heterogeneity and sedimentation rate across cores, we additionally present
 255 the inter-individual age-heterogeneity and implied bioturbation depth for core T86-10P
 256 from the North Atlantic using data published in Lougheed et al. (2018).

257 Estimated age-heterogeneity is again much higher than the measurement error in
 258 most cases, with between replicate standard deviations of 287, 603 and 3208 years, com-
 259 pared to measurement errors of 153, 110, and 304 years (Table 3). The one exception
 260 is core GeoB 10066-7 for which σ_{rep} is only 172 years (+ 40 SE) compared to a mea-
 261 surement error of 185 years. While this could imply no mixing at all ($L = 0$ cm), because
 262 this core has a relatively high sedimentation rate of 29 cm kyr⁻¹, and because the value

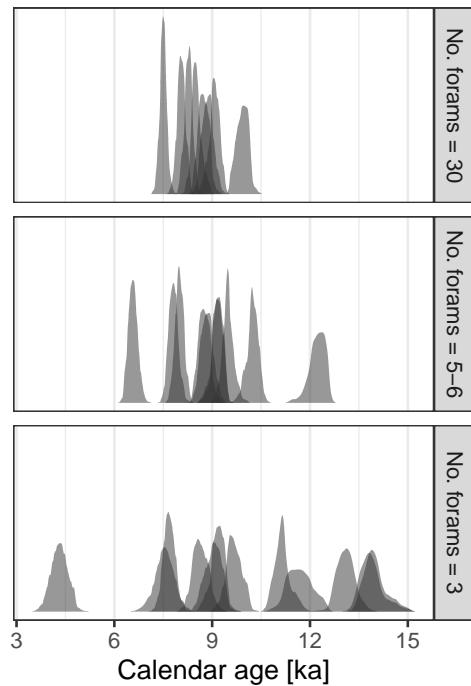


Figure 3. Replicated radiocarbon dates converted to calendar ages from a single 1 cm thick sediment slice, taken at a depth of 21-22 cm, from core SO213-84-2. Each individual density plot shows the probability density function of calendar age obtained by calibrating a radiocarbon age measured on a sample consisting of 3, 5-6 or 30 individual foraminifera (^{14}C age \pm 1 SD) with the Marine13 calibration curve (Reimer et al., 2013). No local adjustment was made to the global marine reservoir effect contained in Marine13.

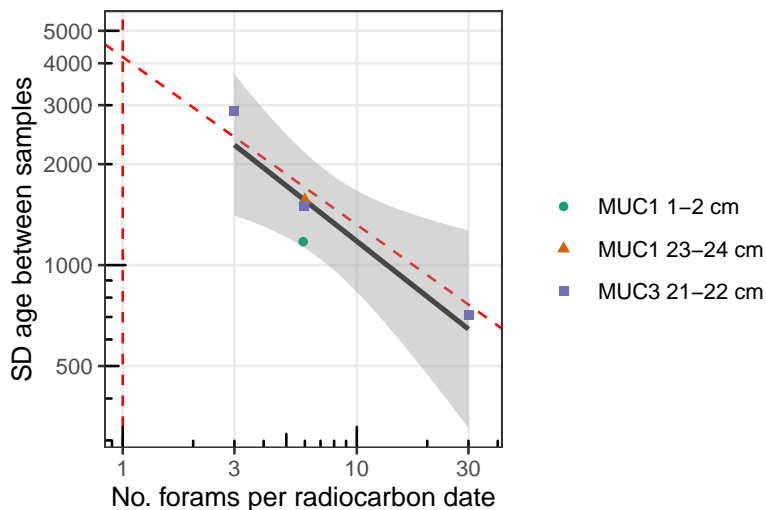


Figure 4. Standard deviation in age between radiocarbon dated samples from core SO213-84-2 as a function of the number of foraminifera they contain. The dashed red lines show extrapolation back to samples of single individual foraminifera assuming the theoretical proportional relationship between standard deviation and the square root of sample size. The samples came from two different multicore tubes of the same deployment.

Table 3. Measured standard deviation between replicated ^{14}C measurements on small- n samples of foraminifera, inferred age-heterogeneity between individual foraminifera and the implied bioturbation depth. n_f is the number of individual foraminifera per radiocarbon measurement, n_{rep} is the number of replicate radiocarbon measurements made on samples of n_f individuals, σ_{rep} is the standard deviation between replicated radiocarbon measurements made from samples from the same sediment slice, $SE_{\sigma_{rep}}$ is the standard error of the estimate of σ_{rep} , σ_{meas} is the reported measurement error, σ_{ind} is the inferred standard deviation in age between individuals. $Bias$ is the estimated proportional bias in σ_{age} due to the exponential relationship between radiocarbon activity and age. Values with the subscript *adj* have been corrected for this bias. s and L are the sediment accumulation rate [cm kyr^{-1}] and inferred bioturbation depth [cm], respectively. Several samples at 11-12 cm from core GeoB 10058-1 had negative radiocarbon dates indicating the presence of modern material and could not be calibrated.

Core	Depth [cm]	n_f	n_{rep}	σ_{rep}	$SE_{\sigma_{rep}}$	σ_{meas}	σ_{ind}	Bias	σ_{indadj}	σ_{slice}	s	L	L_{adj}
GeoB 10054-4	68.0	10	10	287	58	153	766	1.07	820	18	16.3	12.5	13.4
GeoB 10058-1	11.5	5-6	20	98	..	1.10	..	18	16.3
GeoB 10058-1	29.5	5-6	20	603	97	110	1327	1.10	1458	18	16.3	21.7	23.8
GeoB 10066-7	53.0	10	10	172	40	185	526	1.05	553	10	28.9	15.2	16.0
OR1-1218-C2-BC	36.5	5	10	3208	763	304	7142	1.66	11855	169	1.7	12.2	20.2
SO213-84-2	1.5	5-6	10	1187	281	169	2854	1.36	3881	100	2.9	8.3	11.2
SO213-84-2	23.5	5-6	10	1575	374	168	3836	1.36	5218	100	2.9	11.1	15.1
SO213-84-2	21.5	3	12	2895	621	283	4990	1.37	6847	100	2.9	14.4	19.8
SO213-84-2	21.5	5-6	10	1514	359	176	3668	1.36	4989	100	2.9	10.6	14.4
SO213-84-2	21.5	30	8	726	193	152	3888	1.51	5858	100	2.9	11.3	17.0

Table 4. Sediment accumulation rate s (cm kyr⁻¹) and estimated bioturbation depth L (cm) at 4 sites measured in this study, plus one (T86-10P) previously published by Lougheed et al. (2018). SE_s is the standard error of the estimate of s , L_{adj} is the inferred bioturbation depth adjusted for the bias due to the exponential relationship between age and radiocarbon content.

Core/Site	s	SE_s	L	L_{adj}
GeoB 10054-4/58-1	16.3	1.8	16.3	17.7
GeoB 10066-7	28.9	2.4	15.2	16.0
OR1-1218-C2-BC	1.7	0.1	12.2	20.2
SO213-84-2	2.9	0.7	11.1	15.5
T86-10P	2.2	..	10.8	10.8

of σ_{meas} is itself an estimate with its own uncertainty, it is also consistent with mixing of several centimetres. For example, assuming a 15 cm bioturbation depth and given the 10 foraminifera per sample, the expected σ_{rep} would be just 164 years. To provide an upper estimate on the inter-individual age-variance and bioturbation depth for this core, we subtract only the error due to the binomial counting statistics for ¹⁴C/¹²C (45 years), essentially assigning all additional error to age-heterogeneity. Additionally, several samples taken from GeoB 10058-1 at 11.5 cm deep could not be calibrated with Marine13 as they were younger than the minimum 448 radiocarbon years that can be calibrated with Marine13, including some with negative radiocarbon dates indicating the presence of modern material down to at least 11-12 cm.

Across all analysed cores we found a strong negative relationship between sedimentation rate s and inter-individual age-heterogeneity, a clear indication that sediment mixing influences age-heterogeneity. Due to this negative relationship, the implied bioturbation depths for all sets of replicated samples fall within a relatively narrow range of 11.2 - 23.8 cm (Figure 5, Table 3). At the site level, after combining estimates for the same core taken from different depth layers, and combining GeoB 10054-4 and GeoB 10058-1 which come from two sites less than 3 km apart, implied bioturbation depths for the individual sites range from 15.5 - 20.2 cm (Table 4). For core T86-10P, Lougheed et al. (2018) report a mixing depth of 10.8 cm.

The relationship between s and σ_{ind} is only slightly altered by the bias adjustment, which is small compared to other sources of variation in age-heterogeneity. Adjustment is largest for core OR1-1218-C2-BC, for which the simulation study indicated a factor of 1.66, and which has the lowest sedimentation rate and highest estimates of individual age-heterogeneity. The adjustment shifts the implied bioturbation depth from 12.4 to 20.2 cm.

4 Discussion

We found variation in radiocarbon ages between replicated small- n samples of foraminifera that far exceeded the reported machine uncertainty at three of the four sites we examined. Between-replicate age-variation was only within the machine uncertainty for core GeoB 10066-7, which has a comparatively high sedimentation rate of 29 cm kyr⁻¹. Age-heterogeneity also far exceeds measurement error for a fifth core examined by Lougheed et al. (2018). This excess age-variation can be interpreted as within-sediment-layer heterogeneity caused by bioturbation. Assuming the classical Berger and Heath (1968) mixing model, the implied mixing at the five sites is 11-20 cm. This is somewhat higher than the 10 cm often assumed as typical value in literature (Boudreau, 1998) and consider-

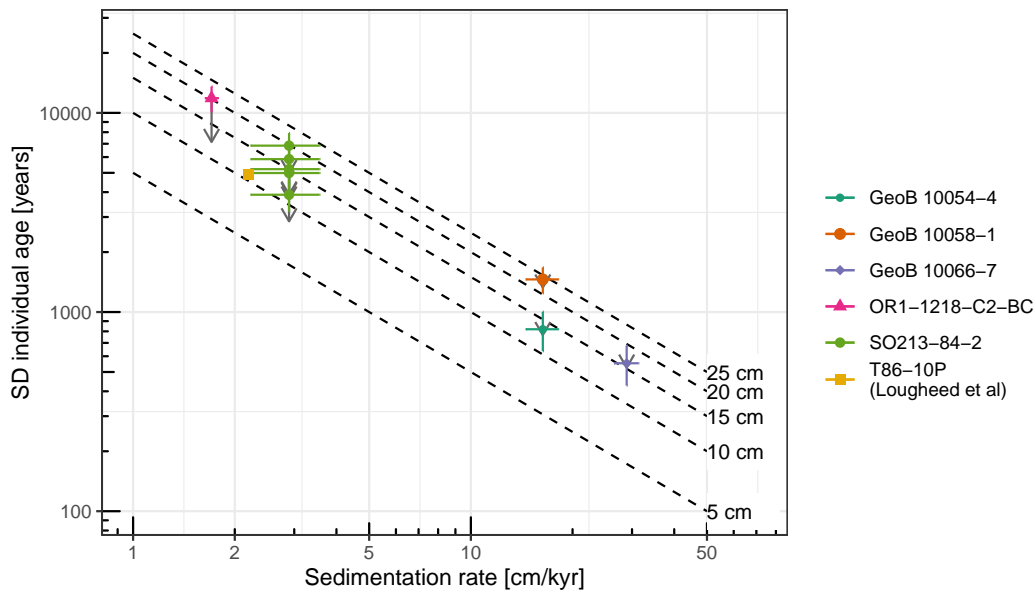


Figure 5. Inferred standard deviation in age between individuals $\sigma_{ind_{adj}}$ plotted against sediment accumulation rate s . Error bars indicate one standard error of the standard deviation and sedimentation rate estimates. The dashed isolines indicate bioturbation depths L consistent with a given sedimentation rate and σ_{ind} . The grey arrows indicate σ_{ind} prior to correcting for the bias due to the exponential relationship between age and radiocarbon content. The bias adjustment is much larger for cores with low sedimentation rates and high estimates of σ_{age} .

298 ably higher than the bioturbation assumed in the interpretation of most paleoclimate
 299 records.

300 Age-heterogeneity of this magnitude has important implications for proxy records
 301 recovered from these cores. The climate signal is strongly smoothed by the mixing to-
 302 gether of time periods, reducing the inferred amplitude of climate variations (e.g., An-
 303 derson, 2001), but, if the proxy measurements are made on small numbers of foraminifera,
 304 records can also become noisier as the signal from different climate states is mixed to-
 305 gether. In extreme cases measurements can include both glacial and interglacial mate-
 306 rial. This noise is especially problematic when the variance itself is of interest, for ex-
 307 ample in individual foraminiferal analyses (Groeneveld et al., 2019; Wit et al., 2013; Koutavas
 308 & Joannides, 2012; Thirumalai et al., 2019, 2013). Estimates of age-heterogeneity from
 309 replicated small- n radiocarbon dates can be used to parametrise proxy forward models
 310 to quantitatively assess this smoothing and noise generation (Lougheed, 2020; Dolman
 311 & Laepple, 2018).

312 A further implication is that radiocarbon dates used for age-depth modelling may
 313 require much larger uncertainties than the reported machine errors that are typically used.
 314 Although they may correctly quantify the uncertainty in the age of the sample, they ig-
 315 nore the uncertainty in how representative the sample may be of mean age of material
 316 at the depth from which it was recovered (Heegaard et al., 2005). The size of this effect
 317 will depend on the bioturbation depth, the sedimentation rate and the sample size. We
 318 can see this effect for the low sedimentation rate multicore SO213-84-2, for which a se-
 319 ries of down-core radiocarbon dates were made in each of 3 sub-cores. These replicated
 320 age-depth series show very little overlap within their reported age-uncertainties (Figure
 321 6a), despite having been measured on samples of approximately 350 foraminifera each.

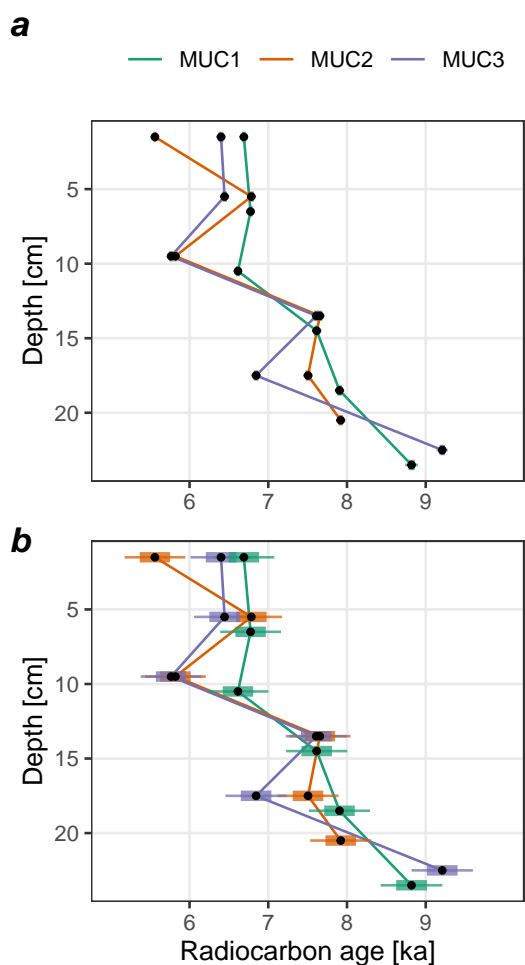


Figure 6. Replicated down-core radiocarbon age estimates for SO213-84-2. Each down-core record corresponds to a separate multicore tube or half tube from the same deployment. Age-uncertainties in subplot (a) are ± 2 times the reported machine error, whereas those in (b) include the inferred σ_{age} between individuals, scaled for samples of 350 individuals.

322 However, adding the expected uncertainty due to age-heterogeneity brings the three down-
 323 core age-depth series into much closer agreement (Figure 6b). Radiocarbon dating small-
 324 *n* samples, either because the sediment material contains only few foraminifera or to save
 325 picking and processing time, risks further inflating this additional error. To guide the
 326 choice of sample size, we have created lookup figures, based on equation 5, for mixing
 327 depths of 5, 10, 15 and 20 cm (Figure 7, S2). These can be used to get a rapid idea of
 328 the number of individual foraminifera per sample required to reduce the additional age-
 329 uncertainty below a desired level, or inversely, given a radiocarbon date we can estimate
 330 the additional hidden uncertainty from age-heterogeneity from the sedimentation rate
 331 and an estimate of the number of individuals in the sample.

332

$$n_f = \left(\frac{1000L}{s \cdot \sigma_{rep}} \right)^2 \quad (5)$$

333

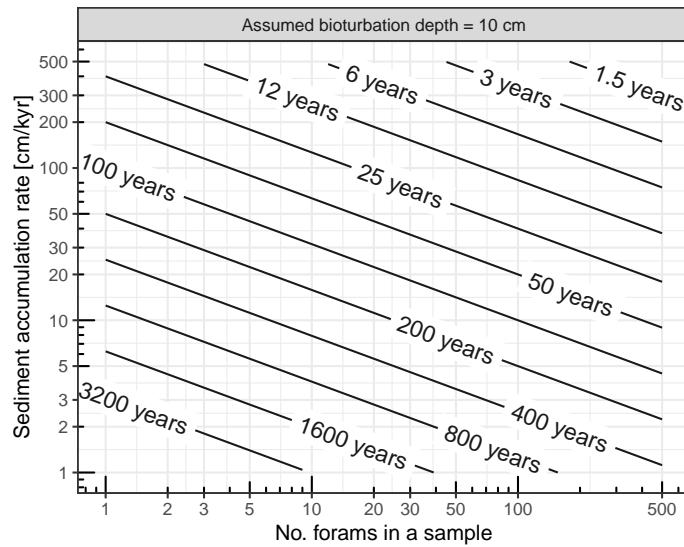


Figure 7. A reference chart to obtain estimates of the additional age-uncertainty σ_{age} for a sample measured on a given number of foraminifera, from the sedimentation rate of the core s , and assuming a bioturbation depth L of 10 cm. Or alternatively, an estimate of the number of foraminifera per sample needed to reduce σ_{age} below a given level. E.g. for a core with $s = 5 \text{ cm kyr}^{-1}$, to get the additional age-uncertainty below 200 years you need at least 100 foraminifera; if s were 20 cm kyr^{-1} you would need only 6-7 foraminifera. The σ_{age} values of the isolines are proportional to L , so if a larger, 20 cm, bioturbation depth is suspected, double the isoline values. Note however, altering the mass of material processed and measured may also influence the reported instrument error - and the characteristic sizes of different foraminiferal taxa will impose their own constraints on the number of specimens required.

333

4.1 The Physical Mixing Process and Outliers

334

335

336

337

338

339

340

341

342

343

344

345

346

347

348

349

350

351

352

The concept of a bioturbation depth is an obvious simplification; however, as the age-heterogeneity is related to the sedimentation rate regardless of the precise mixing process (Matisoff, 1982), the specific mixing model assumed is not particularly important for the main conclusions here. We can still however question the extent to which our measured radiocarbon dates are consistent with the Berger and Heath (1968) mixing model. In contrast to Lougheed et al. (2018), who estimated that around 10% of their foraminifera had ages inconsistent with a simple mixing model, we found very few extreme outlying dates which might be evidence of unusually deep mixing events like *Zoophycos* burrows (Küssner et al., 2018). However, as we dated samples containing multiple foraminifera, individuals with aberrant ages may be hidden, as every distribution will converge towards a Gaussian distribution as the number of individuals increases (Figure S3). Therefore it is unclear the extent to which additional disturbance by *Zoophycos*, or other deep mixing mechanisms, contribute to the age-heterogeneity we measure. The single clear outlier we did obtain was measured on just three individuals, and was too young by about 5000 years in a core with sedimentation rate of 2.9 cm kyr⁻¹ (core SO213-84-2). This implies a relative displacement of approximately 43.5 cm for one of the three foraminifera, which would be consistent with the known size of *Zoophycos* burrows (Wetzel & Werner, 1980). Additional displaced individuals hidden inside multi-individual measurements would mean that we have overestimated the depth of the well mixed layer.

353

354

355

356

357

358

359

360

361

362

The specific form of mixing and its resulting probability distribution of ages does have implications for the bias generated by the exponential relationship between age and the ¹⁴C/¹²C ratio. We calculated biases for the highly skewed exponential distribution resulting from the Berger and Heath (1968) mixing model; less skewed distributions, resulting for example from incomplete mixing or a smooth transition between the mixed layer and the unmixed sediment, will generate a smaller bias. Therefore our bias correction which assumes an exponential distribution may be too strong and probably represents an upper limit. This bias could potentially be eliminated by dating individual larger foraminifera (e.g., Lougheed et al., 2018), which would also remove the issue of hidden outliers.

363

364

365

366

367

368

369

370

In principle, $\Delta^{14}\text{C}$ variations across the water column also cause some apparent age-heterogeneity due to differences in the calcification depth of the individual foraminifera. However, even assuming a strong $\Delta^{14}\text{C}$ gradient (0.2 permille change per meter) and a highly variable calcification depth (uniform probability of calcifying between 0 and 100 m), the resulting heterogeneity ($\sigma = 50$ years) is small compared to the age-heterogeneity found in this study. Over most of the ocean the $\Delta^{14}\text{C}$ gradient is weaker than this (Key, 2001), and individual foraminifera may incorporate carbon over a range of depths during their calcification.

371

4.2 Practical Considerations When Applying This Method

372

373

374

375

376

We have demonstrated the use of small- n radiocarbon measurements to estimate site and core-depth specific bioturbational mixing. This knowledge is especially important when a high-resolution analysis or the analysis of individual foraminifera (IFA) is planned, and it is our hope that bioturbation estimates will become routine in these applications. However, there are some practical considerations when applying this method.

377

378

379

380

381

382

383

Firstly, the estimation only works if the age-heterogeneity is larger than the measurement error. For the data presented here, measurement error ranged from about 80 to 400 years. At sedimentation rates below about 2 cm kyr⁻¹, age-heterogeneity from bioturbation will far exceed this measurement error, even for relatively small bioturbation depths. However, as s rises, the expected age-heterogeneity between individuals (Figure 5, dashed lines), or samples (Figure 7, contour lines), falls rapidly. Furthermore, for many foraminifera taxa, single specimens cannot be dated, even with MICADAS, and

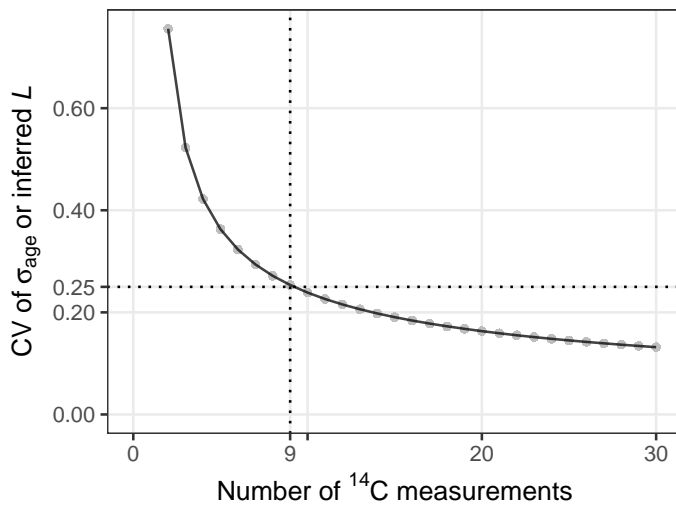


Figure 8. Coefficient of variation for estimates of σ_{age} or the implied bioturbation depth L as a function of the number of dated samples n_{rep} . Dashed lines indicate that for 9 replicated ^{14}C measurements there would be a 25% uncertainty in the estimated values of σ_{age} and L .

384 so the approach of dating small- n samples has to be used - reducing the signal of age-
 385 heterogeneity by a factor of n_f .

386 Secondly, the uncertainty, or standard error (SE), of a standard deviation depends
 387 on the number of samples measured (Equation 6), hence a sufficient number of small-
 388 n samples needs to be measured in order to get a reliable estimate of σ_{ind} , and in turn
 389 to estimate L with a given precision. For example, with approximately 9 samples, the
 390 proportional uncertainty (or coefficient of variation) of the standard deviation is approx-
 391 imately 1/4 (Figure 8), therefore with true bioturbation depths of 10 or 2 cm we would
 392 expect estimates of 10 \pm 2.5 cm or 2 \pm 0.5 cm respectively.

393
$$SE_{\sigma_{ind}} = \frac{\sigma_{ind}}{\sqrt{2(n_s - 1)}} \quad (6)$$

394 5 Conclusions

395 An awareness of bioturbation and its potential influence on sedimentary proxy records
 396 due to the age-heterogeneity it causes is not new (e.g., Schiffelbein, 1985; Andree, 1987;
 397 Keigwin & Guilderson, 2009; Steiner et al., 2016; Goreau, 1980); however, it has only re-
 398 cently become possible to directly measure the age-heterogeneity in sediment slices of
 399 the medium that is radiocarbon dated, e.g. foraminifera. We measured age-heterogeneities
 400 that imply much deeper mixing than is typically assumed in the paleo-climate literature.
 401 At the same time, we found that between core variation in age-heterogeneity could largely
 402 be explained by sedimentation rates, which implies a relatively consistent mixed layer
 403 depth. It is conceivable that the "paleo" bioturbation depth is larger and less variable
 404 than measurements of contemporary bioturbation depths would imply (e.g., Solan et al.,
 405 2019), as integrated over time, a long period of shallow mixing would be obliterated by
 406 a subsequent period of deep mixing; where "long" is relative to the sedimentation rate.
 407 The availability of small- n radiocarbon dating will allow us to assess how consistent bio-
 408 turbation depths really are, in addition to obtaining independent estimates of age-heterogeneity
 409 to aid our interpretation of proxy climate records.

410 **Acknowledgments**

411 We thank the scientists and crew members on board the research vessels R/V Sonne and
 412 Ocean Researcher 1 who helped with sample retrieval, especially M. Mohtadi (all GeoB
 413 cores), F. Lamy (SO213-84-2), and C.-C. Su and A. Zuhr (OR1-1218-C2-BC). Thanks
 414 are owed to R. De Pol-Holz for help with radiocarbon measurements carried out at Keck-
 415 Carbon Cycle AMS facility, and to H. Grotheer, E. Bonk and T. Gentz who carried out
 416 the MICADAS AMS analyses. N. Behrendt and L. Kafemann assisted with sample prepa-
 417 ration. T. Ronge is acknowledged for discussion, without implying agreement on what
 418 is written in this manuscript.

419 This is a contribution to the SPACE ERC project; this project has received fund-
 420 ing from the European Research Council (ERC) under the European Union’s Horizon
 421 2020 research and innovation programme (grant agreement no. 716092). Additionally,
 422 this work was supported by German Federal Ministry of Education and Research (BMBF)
 423 as Research for Sustainability initiative (FONA); www.fona.de through Palmod project
 424 (FKZ: 01LP1509C). Samples from core SO213-84-2 were processed and analysed while
 425 Sze Ling Ho was supported by the Initiative and Networking Fund of the Helmholtz As-
 426 sociation Grant VG-NH900.

427 Radiocarbon dates have been submitted to Pangaea (www.pangaea.de - DOI pend-
 428 ing). Additionally, the data and R code to reproduce the analyses are supplied as Sup-
 429 porting Material to this manuscript (Data Set S1).

430 **References**

431 Anderson, D. M. (2001). Attenuation of millennial-scale events by biotur-
 432 bation in marine sediments. *Paleoceanography*, 16(4), 352–357. doi:
 433 10.1029/2000PA000530

434 Andree, M. (1987). The Impact of Bioturbation on AMS 14C Dates On Handpicked
 435 Foraminifera: A Statistical Model. *Radiocarbon*, 29(2), 169–175. doi: 10.1017/
 436 S0033822200056927

437 Berger, W. H., & Heath, G. R. (1968). Vertical mixing in pelagic sediments. *Journal*
 438 *of Marine Research*, 26(2), 134–143.

439 Boudreau, B. P. (1998). Mean mixed depth of sediments: The wherefore and the
 440 why. *Limnology and Oceanography*, 43(3), 524–526. doi: 10.4319/lo.1998.43.3
 441 .0524

442 Dolman, A. M., Kunz, T., Groeneveld, J., & Laepple, T. (2020). Estimating the
 443 timescale-dependent uncertainty of paleoclimate records – a spectral
 444 approach. Part II: Application and interpretation. *Climate of the Past Discus-*
 445 *sions*, 1–22. doi: 10.5194/cp-2019-153

446 Dolman, A. M., & Laepple, T. (2018). Sedprox: A forward model for sediment-
 447 archived climate proxies. *Climate of the Past*, 14(12), 1851–1868. doi: 10
 448 .5194/cp-14-1851-2018

449 Goreau, T. J. (1980). Frequency sensitivity of the deep-sea climatic record. *Nature*,
 450 287(5783), 620. doi: 10.1038/287620a0

451 Groeneveld, J., Ho, S. L., Mackensen, A., Mohtadi, M., & Laepple, T. (2019).
 452 Deciphering the variability in Mg/Ca and stable oxygen isotopes of indi-
 453 vidual foraminifera. *Paleoceanography and Paleoclimatology*, 0(ja). doi:
 454 10.1029/2018PA003533

455 Guinasso, N. L. G., & Schink, D. R. (1975). Quantitative Estimates of Biological
 456 Mixing Rates in Abyssal Sediments. *Journal of Geophysical Research*, 80(21),
 457 PP. 3032-3043. doi: 197510.1029/JC080i021p03032

458 Haslett, J., & Parnell, A. (2008). A simple monotone process with appli-
 459 cation to radiocarbon-dated depth chronologies. *Journal of the Royal*
 460 *Statistical Society: Series C (Applied Statistics)*, 57(4), 399–418. doi:
 461 10.1111/j.1467-9876.2008.00623.x

- 462 Hebbeln, D., & cruise participants. (2006). *Report and preliminary results of RV*
 463 *Sonne Cruise SO-184, Pabesia, Durban (South Africa) - Cilacap (Indonesia) -*
 464 *Darwin (Australia), July 8th - September 13th, 2005* (Vol. 246). Department of
 465 Geosciences, Bremen University.
- 466 Heegaard, E., Birks, H. J. B., & Telford, R. J. (2005). Relationships between
 467 calibrated ages and depth in stratigraphical sequences: An estimation pro-
 468 cedure by mixed-effect regression. *The Holocene*, 15(4), 612–618. doi:
 469 10.1191/0959683605hl836rr
- 470 Keigwin, L. D., & Guilderson, T. P. (2009). Bioturbation artifacts in zero-age sedi-
 471 ments. *Paleoceanography*, 24(4), PA4212. doi: 10.1029/2008PA001727
- 472 Key, R. (2001). Radiocarbon. In *Encyclopedia of Ocean Sciences* (pp. 2338–2353).
 473 Elsevier. doi: 10.1006/rwos.2001.0162
- 474 Koutavas, A., & Joanides, S. (2012). El Niño–Southern Oscillation extrema in the
 475 Holocene and Last Glacial Maximum. *Paleoceanography*, 27(4), PA4208. doi:
 476 10.1029/2012PA002378
- 477 Kunz, T., Dolman, A. M., & Laepple, T. (2020). A spectral approach to es-
 478 timating the timescale-dependent uncertainty of paleoclimate records –
 479 Part 1: Theoretical concept. *Climate of the Past*, 16(4), 1469–1492. doi:
 480 10.5194/cp-16-1469-2020
- 481 Küssner, K., Sarnthein, M., Lamy, F., & Tiedemann, R. (2018). High-resolution
 482 radiocarbon records trace episodes of Zoophycos burrowing. *Marine Geology*,
 483 403, 48–56. doi: 10.1016/j.margeo.2018.04.013
- 484 Lea, D. W. (2014). Elemental and Isotopic Proxies of Past Ocean Temperatures. In
 485 *Treatise on Geochemistry* (Second ed., Vol. 1-16, pp. 373–397). Elsevier.
- 486 Lougheed, B. C. (2020). SEAMUS (v1.20): A $\Delta^{14}\text{C}$ -enabled, single-specimen sed-
 487 iment accumulation simulator. *Geoscientific Model Development*, 13(1), 155–
 488 168. doi: 10.5194/gmd-13-155-2020
- 489 Lougheed, B. C., Metcalfe, B., Ninnemann, U. S., & Wacker, L. (2018). Moving be-
 490 yond the age–depth model paradigm in deep-sea palaeoclimate archives: Dual
 491 radiocarbon and stable isotope analysis on single foraminifera. *Climate of the*
 492 *Past*, 14(4), 515–526. doi: 10.5194/cp-14-515-2018
- 493 Matisoff, G. (1982). Mathematical models of bioturbation. In P. L. McCall &
 494 M. J. S. Tevesz (Eds.), *Animal-sediment relations: The biogenic alteration of*
 495 *sediments* (pp. 289–330). New York: Springer.
- 496 Nürnberg, D., Bijma, J., & Hemleben, C. (1996). Assessing the reliability of magne-
 497 sium in foraminiferal calcite as a proxy for water mass temperatures. *Geochim-*
 498 *ica et Cosmochimica Acta*, 60(5), 803–814. doi: 10.1016/0016-7037(95)00446
 499 -7
- 500 Officer, C., & Lynch, D. (1983). Determination of mixing parameters from tracer
 501 distributions in deep-sea sediment cores. *Marine Geology*, 52(1-2), 59–74. doi:
 502 10.1016/0025-3227(83)90021-X
- 503 R Core Team. (2019). *R: A language and environment for statistical computing*. Vi-
 504 enna, Austria.
- 505 Reimer, P. J., Bard, E., Bayliss, A., Beck, J. W., Blackwell, P. G., Ramsey, C. B.,
 506 ... van der Plicht, J. (2013). IntCal13 and Marine13 Radiocarbon Age Cal-
 507 ibration Curves 0–50,000 Years cal BP. *Radiocarbon*, 55(4), 1869–1887. doi:
 508 10.2458/azu_js_rc.55.16947
- 509 Rosenthal, Y., Lohmann, G. P., Lohmann, K. C., & Sherrell, R. M. (2000). Inco-
 510 rporation and preservation of Mg in Globigerinoides sacculifer: Implications for
 511 reconstructing the temperature and 18O/16O of seawater. *Paleoceanography*,
 512 15(1), 135–145. doi: 10.1029/1999PA000415
- 513 Ruff, M., Szidat, S., Gäggeler, H. W., Suter, M., Synal, H. A., & Wacker, L. (2010).
 514 Gaseous radiocarbon measurements of small samples. *Nuclear Instruments and*
 515 *Methods in Physics Research Section B: Beam Interactions with Materials and*
 516 *Atoms*, 268(7), 790–794. doi: 10.1016/j.nimb.2009.10.032

- 517 Schiffelbein, P. (1985). Calculation of error measures for deconvolved deep-sea strati-
 518 graphic records. *Marine Geology*, *65*(3), 333–342. doi: 10.1016/0025-3227(85)
 519 90063-5
- 520 Schiffelbein, P., & Hills, S. (1984). Direct assessment of stable isotope variabil-
 521 ity in planktonic foraminifera populations. *Palaeogeography, Palaeoclimatology,*
 522 *Palaeoecology*, *48*(2), 197–213. doi: 10.1016/0031-0182(84)90044-0
- 523 Solan, M., Ward, E. R., White, E. L., Hibberd, E. E., Cassidy, C., Schuster, J. M.,
 524 ... Godbold, J. A. (2019). Worldwide measurements of bioturbation intensity,
 525 ventilation rate, and the mixing depth of marine sediments. *Scientific Data*,
 526 *6*(1), 58. doi: 10.1038/s41597-019-0069-7
- 527 Steiner, Z., Lazar, B., Levi, S., Tsroya, S., Pelled, O., Bookman, R., & Erez, J.
 528 (2016). The effect of bioturbation in pelagic sediments: Lessons from ra-
 529 dioactive tracers and planktonic foraminifera in the Gulf of Aqaba, Red
 530 Sea. *Geochimica et Cosmochimica Acta*, *194*, 139–152. doi: 10.1016/
 531 j.gca.2016.08.037
- 532 Teal, L., Bulling, M., Parker, E., & Solan, M. (2010). Global patterns of biotur-
 533 bation intensity and mixed depth of marine soft sediments. *Aquatic Biology*,
 534 *2*(3), 207–218. doi: 10.3354/ab00052
- 535 Thirumalai, K., DiNezio, P. N., Tierney, J. E., Puy, M., & Mohtadi,
 536 M. (2019). *An El Niño mode in the glacial Indian Ocean?*
 537 <https://agupubs.onlinelibrary.wiley.com/doi/abs/10.1029/2019PA003669>.
 538 doi: 10.1029/2019PA003669
- 539 Thirumalai, K., Partin, J. W., Jackson, C. S., & Quinn, T. M. (2013). Statistical
 540 constraints on El Niño Southern Oscillation reconstructions using individual
 541 foraminifera: A sensitivity analysis. *Paleoceanography*, *28*(3), 401–412. doi:
 542 10.1002/palo.20037
- 543 Thomson, J., Cook, G. T., Anderson, R., MacKenzie, A. B., Harkness, D. D., &
 544 McCave, I. N. (1995). Radiocarbon Age Offsets in Different-Sized Carbon-
 545 ate Components of Deep-Sea Sediments. *Radiocarbon*, *37*(2), 91–101. doi:
 546 10.1017/S0033822200030526
- 547 Tiedemann, R., Lamy, F., Molina-Kescher, M., Tapia Arroyo, R., Poggemann,
 548 D. W., & Nürnberg, D. (2014). *FS Sonne Fahrtbericht / Cruise Report*
 549 *SO213 - SOPATRA: South Pacific Paleoceanographic Transects - Geodynamic*
 550 *and Climatic Variability in Space and Time, Leg 1: Valparaiso/Chile - Val-*
 551 *paraiso/Chile, 27.12.2010 - 12.01.2011 and Leg 2: Valparaiso/Chile - Wellin-*
 552 *ton/New Zealand, 12.01.2011 - 07.03.2011* (Report). doi: 10.2312/cr_so213
- 553 Trauth, M. H., Sarnthein, M., & Arnold, M. (1997). Bioturbational mixing depth
 554 and carbon flux at the seafloor. *Paleoceanography*, *12*(3), 517–526. doi: 10
 555 .1029/97PA00722
- 556 Wacker, L., Bonani, G., Friedrich, M., Hajdas, I., Kromer, B., Nemeč, N., ... Vock-
 557 enhuber, C. (2010). MICADAS: Routine and High-Precision Radiocarbon
 558 Dating. *Radiocarbon*, *52*(2), 252–262. doi: 10.1017/S0033822200045288
- 559 Wetzel, A., & Werner, F. (1980). Morphology and ecological significance of Zoophy-
 560 cos in deep-sea sediments off NW Africa. *Palaeogeography, Palaeoclimatology,*
 561 *Palaeoecology*, *32*, 185–212. doi: 10.1016/0031-0182(80)90040-1
- 562 Wheatcroft, R. A. (1992). Experimental tests for particle size-dependent bioturba-
 563 tion in the deep ocean. *Limnology and Oceanography*, *37*(1), 90–104. doi: 10
 564 .4319/lo.1992.37.1.0090
- 565 Wit, J., Reichart, G., & Ganssen, G. (2013). Unmixing of stable isotope signals
 566 using single specimen $\delta^{18}\text{O}$ analyses. *Geochemistry, Geophysics, Geosystems*,
 567 *14*(4), 1312–1320. doi: 10.1002/ggge.20101